International Transaction of Electrical and Computer Engineers System, 2014, Vol. 2, No. 3, 98-106
Available online at http://pubs.sciepub.com/iteces/2/3/4

DOI:10.12691/iteces-2-3-4

Evaluation of the Voltage Stability of a Radial Distribution System having V2G Facilities

Uwakwe C. Chukwu[1,*], Satish M. Mahajan[2]

[1]Department of Industrial & Electrical Engineering Technology of South Carolina State University, U.S.A.
[2]Electrical and Computer engineering, Tennessee Technological University, Cookeville, TN, U.S.A.
*Corresponding author: uchukwu@scsu.edu

Received December 26, 2013; Revised May 29, 2014; Accepted June 06, 2014

Abstract The penetration of V2G into the distribution system is expected to impact the way power systems are being operated. Voltage instability in the distribution system is a growing problem, and is associated with rapid voltage drops due to heavy load demand that may occur during uncoordinated and simultaneous charging of V2G units during peak hours of a typical day**.** This is a pressing issue since the next generation electric distribution system may exhibit a high level of volatility due to V2G penetration. In this paper, the impact of V2G parking lots on voltage stability of a radial distribution network is investigated. IEEE 13 Node test feeder network was modeled in the RDAP. Load flow results were applied to the voltage stability index. Results show that for a given penetration level, 3-phase and system-wide V2G integration results in an improved voltage stability than a 1-phase V2G integration. Results also indicate that using V2G parking lots to inject reactive power will have an improved impact on the voltage stability of the system than injecting a real power into the system. These results could be useful for real-time applications as well as for power system operators and planners dealing with an increasing influx of V2Gs in the distribution system.

Keywords: *radial distribution, smart-grid, power demand/injection, voltage collapse, voltage stability, V2G*

Cite This Article: Uwakwe C. Chukwu, and Satish M. Mahajan, "Evaluation of the Voltage Stability of a Radial Distribution System having V2G Facilities." *International Transaction of Electrical and Computer Engineers System*, vol. 2, no. 3 (2014): 98-106. doi: 10.12691/iteces-2-3-4.

1. Introduction

The distribution system in the next few years may become more unpredictable due to the highly precarious nature of the arrival and departure of vehicle-to-grid (V2G) vehicles at the V2G parking lots. The system is further made more volatile considering the fact that electricity demand profiles due to customer charging of V2G units is also unpredictable. The random *plug-in and play* of V2G vehicles at residential homes, private structures and vehicle fleet companies is expected to affect the overall performance of the distribution system. The charging and discharging of V2G batteries due to customers service choice create a bipolar characteristic at the load centers, and will definitely alter the behavior of the distribution system. This unpredictability and uncontrollability of demand load profiles may cause the next generation electric distribution system to exhibit a high level of volatility and undesirable performance if proper system planning is not done *ab initio*. It is expected that high penetration of V2G into the distribution system in the scenario of power system expansion and increasing grid interconnectivity may make the entire electric power systems more complex than ever, thereby leading to a state of potentially incredible unreliability and instability. Therefore, there is a need to study: how a V2G penetration may affect the voltage stability of the distribution system. Earlier work studied the effect of V2G in a distribution system (assuming a balanced condition) [1,2]. No known previous work has been done to investigate the effect of V2G on the voltage stability of an unbalanced distribution system. An attempt is made to fill this void through this work.

The importance of this study is highlighted in the real-time requirements of a smart-grid structure. Power systems for real-time applications must satisfy timing constraints associated with changing system state, in addition to maintaining accurate security information of the system. Smart grid applications provide an excellent opportunity to better manage the voltage stability of the power system. With the aid of supervisory control and data acquisition (SCADA), global positioning system, and intelligent electronic devices, it is possible to capture power system data, and give an instantaneous snapshot of the real-time monitoring of the network's voltage stability status.

This paper is organized as follows: - In section II, voltage stability in V2G scenario is presented, voltage stability model is presented in section III. Numerical results are presented in section IV, and conclusions are presented in section V.

2. Voltage Stability in a V2G Scenario

In the past twenty eight years or so, research community has seen a growing interest and investigation in the voltage instability problems [3]. Factors driving the power system into voltage instability are heavy loading, complexity of interconnected grids, and penetration of new technologies (e.g., V2G). The heart of the voltage stability problem is the inability of the system to meet its reactive power demands [4]. A detailed bibliography on voltage stability has been reported in [3]. A detailed review of voltage stability focusing on network equivalent methodology was discussed in [5]. The loading and power injection by V2G affects voltage stability of an electrical network, because electric vehicles exhibits high level of variability of real and reactive power- both during charging and discharging operations. This impact of this variability characteristic is studied in this paper.

An early prediction of voltage instability is indispensable in a power system operation, and can ameliorate reliability and economical problems. Several contributions have been made in terms of static voltage stability analysis tools, namely: singularity of power flow Jacobian [6,7], singular value decomposition technique or eigenvalue analysis [6,7], continuation power flow method [6,8]; sensitivity factors [9], singular value index [7,9], voltage collapse proximity indicator [9], reactive power margin [6], voltage stability L-index [10,11], and voltage stability index for radial distribution networks [11,12]. Application of load shading and capacitors for voltage stability enhancement were considered in [11,14]. This work deals with static voltage stability index evaluation in a radial distribution system.

3. Modeling Voltage Stability of a Radial Distribution Network

The VSI formulation utilized in this research is the method described in [14]. Considering Figure 1, the VSI for node *m* (VSI_m) is computed as [14]

$$VSI_m = \left(2\frac{V_m}{V_k}\cos(\delta_k - \delta_m) - 1\right)^2 \quad (1)$$

where V_m is the node voltage at node *m* and V_k is the node voltage at node *k*; δ_k is the voltage angle at node *k*, while δ_m is the voltage angle at node *m*. The model (1) is linear in the entire operating region. For a balanced system, the magnitude of VSI varies between unity (at no load) and zero (at voltage collapse). The voltage stability margin (VSM) of such a feeder depicted in Figure 1 is given by [12,14]

$$VSM_{k,m} = \prod_{i\in\Omega} VSI \quad (2)$$

where α is a set of branches or laterals constituting the enter length of each feeder, starting from the source bus to the receiving end bus. A feeder with the lowest value of the VSM is considered as the weakest feeder of the system, and is defined as [12]

$$VSM_{sym} = \min\left(VSM_1, VSM_2, ..., VSM_j\right) \quad (3)$$

where *j* is the number of feeders (or laterals of a feeder) in the system. The system VSM (VSM_{sys}) is an indicator of the nearness of the system to voltage collapse. Equations (1)-(3) may provide algorithmic basis for real-time computation of the distribution network.

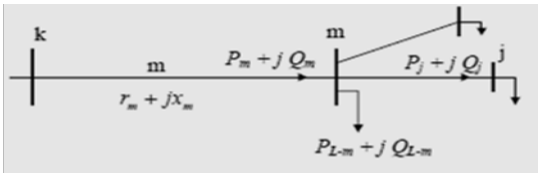

Figure 1. Typical Radial Distribution System [14]

In this work, V2G penetration is defined as the percentage of the substation electric power capacity. For instance, 50% penetration in a system with 5 MW substation capacity means a cumulative V2G capacity of 2500 kW. The impact of 1-phase and 3-phase V2G interconnection at given penetration level was investigated with respect to impacts on three phases of the system. Seven case studies presented in Table 1 were used to investigate the impacts that different V2G penetration levels may have on the test feeder system. In Table 1, V2G are either charging or discharging.

Table 1. Case Studies (*50% ≡ 2500 kW or 2500 kvar)

Case	%V2G Penetration		Comment
	Discharging Mode	Charging mode	
1.	0	0	Original System (Base Case)
2.	0	*50	All V2G consuming only kW
3.	50	0	All V2G injecting kW
4.	50	50	50% of V2G injecting kW, 50% Consuming kW
5.	50	50	50% of V2G injecting KVAr, 50% Consuming kW
6.	50	0	All V2G injecting KVAr
7.	50/50	0	50% of V2G injecting KVAr, 50% and other 50% injecting kW

When discharging, either kW or kvar is injected to the feeder (hence V2G parking lots behaves like a power source) but consumes only kW when charging (load source). All appearances of 'Case 1' in the results presented are merely to establish a quick comparison between base case (Case 1) and other cases. A V2G parking lot with power electronic provision was assumed for power injection. In order to exhaustively explore possible system operational cases in a real life scenario, a comprehensive study of the different penetration levels of V2G was performed with respect to the following ten scenarios (presented in Table 2). Each scenario was further investigated in the context of the seven case studies presented in Table 1.

Table 2. Scenario Studies (*50% ≡ 2500 kW or 2500kvar)

Scenario	Activities
1	V2G injecting kVAr/kW or demanding kW on Phase A
2	V2G injecting kVAr/kW or demanding kW on Phase B
3	V2G injecting kVAr/kW or demanding kW on Phase C
4	V2G injecting kVAr/kW or demanding kW on 3-Phase
5	V2G consuming 2500kW on entire system at all load buses
6	V2G injecting 2500kW to entire system at all load buses
7	V2G consuming 2500kW and injecting 2500kVAr in entire system
8	V2G injecting 2500kVAr to entire system at load buses
9	V2G simultaneously injecting 2500kW and 2500kVAr to entire system
10	a. V2G consuming kW in multiples of system kW load b. V2G injecting kW in multiples of system kW load c. V2G injecting kVAr in multiples of system kVAr load

The above 10 scenarios may be grouped into three categories, namely: Category A, Category B, or Category C. Thus, the categories are:

Scenario-1, Scenario-2, Scenario-3, Scenario-4 } Category A: {case1, case 2, case 3, case 4, case 5, case 6, case 7}

Scenario-5, Scenario-6, Scenario-7, Scenario-8, Scenario-9 } Category B: [V2G interconnected to all load buses supplying/consuming 2500 kW and 2500 kWAr (1-phase and 3-phase alike)]

Scenario-10 } *Category C*: [V2G interconnected to all load buses supplying or consuming power in multiplesof base load (1-phase and 3-phase alike)]

4. Numerical Results

The IEEE 13 Node Test Feeder network and data used in this study are presented in [13]. In order to clearly see the effect of V2G on the distribution systems, the voltage regulator and shunt capacitors in the networks were disabled (because these devices also affect voltage quantities). RDAP program was used for load flow analysis of the test system. The load flow results were used to compute the system's voltage stability. The impact of different penetration levels of V2G on the system voltage profile, VSI, and VSM were investigated. The 7 cases in Table 1 and 10 scenarios in Table 2 were applied. The aim was to investigate how the different cases and scenarios affect voltage stability of the distribution network. We assumed a steady state (i.e., a snap-shop of what is expected to happen in the system under the different cases and scenarios investigated). The modeling of the EV load is assumed to be PQ Load model representation.

4.1. Category A: Scenario-1

From Table 2, scenario 1 is a 1-phase operation. The IEEE 13 Node Test Feeder data shows that N_652 is a phase_A lateral. Hence, a 1-phase V2G parking lots unit was interconnected at node N_652 to study the effect of installing V2G to Phase A on the entire system. For each case- in all the scenarios- the kW and kvar injections from the V2G unit (or the kW demand by the V2G) were made at the V2G interconnection node (in this case, N_652).

4.1.1. Voltage Stability Index

VSI is used to identify nodes that are on the verge of voltage collapse with respect to the existing load condition (VS1 nearer to zero is more prone to voltage collapse). The VSI for the IEEE 13 Node Test Feeder for V2G Interconnection at Phase A is presented in Figure 2. The VSI computation was done using (1). The result shows that significant changes in VSI for different cases took place at node 632 and node 671 of the main feeder (each of the nodes supply two loaded laterals: 671-684-611 and 671-692, and 675 from node 671; 632-645-646 and 632-633, and 634 from 632).

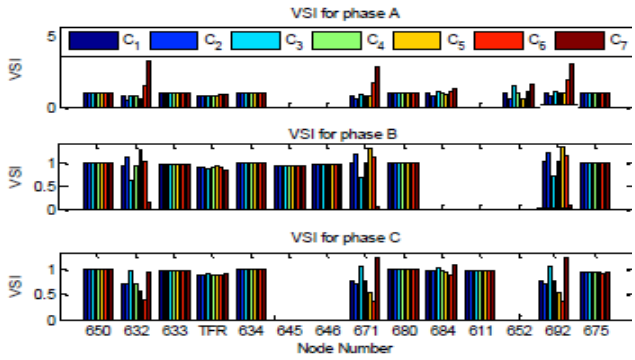

Figure 2. VSI for IEEE 13 Test Feeder for V2G Interconnection at Phase A

It should be noted that node 680 and the source node do not have laterals, and therefore have fairly constant VSI for all the 3-phase cases considered. Additionally, major changes in VSI took place at the 1-phase bus at node 652, where the V2G is interconnected, and at bus 684 (that feeds the sub-lateral 684-652). It can also be observed that Case 3, Case 6 and Case 7 resulted in improved VSI in 2-phase circuits. Based on these observations, it is evident that interconnecting V2G at node 652 Phase A significantly affected the VSI of the main feeder nodes as well as the nodes of the lateral that lead to where the V2G is interconnected. Furthermore, operating V2G to inject either kW or kvar, or both resulted in improved VSI in at the most two phase lines.

4.1.2. Voltage Stability Margin

The VSM was computed using (2) to quantify the nearness of the feeder system to voltage collapse. The single line diagram of the IEEE 13 Node Test Feeder system indicates that the system has one main feeder and 5 laterals) [13]. For the purpose of clarity in analysis, the following set of laterals is defined: Feeder 1 (F_1): α_1 = {650-632-671-680}, Lateral 1 (L_1): α_2 = {650-632-633-634}, Lateral 2 (L_2): α_3 = {650-632-645-646}; Lateral 3 (L_3): α_4 = {650-632-671-692-675}, Lateral 4 (L_4): α_5 = {650-632-671-684-611}, and Lateral5 (L_5): α_6 = {650-632-671-684-652}.

The results presented in Figure 3 show the feeder VSM for the seven cases under 3-phase study. For all the six laterals, significant impacts on VSM are made in all cases with the highest impact on Phase A (note scale of the plots). The extreme magnitude of VSM in Phase A was at a large penalty in the VSM of Phase B (same thing happened in VSI, Figure 2). Because 3-phase feeder is considered, it was appropriate to define the VSM of a feeder line segment as the lowest value of VSM for the three phases of a feeder or lateral segment. Hence, The Feeder VSM, $VSM_{fdr,k}$, is defined as

$$VSM_{fdr,k} = \min\left(VSM_{fdr,k}^{abc}\right) \quad (4)$$

where $VSM_{fdr,k}^{abc}$ is the VSM of phase *a*, *b*, *c* for k^{th} Feeder or lateral. From (4), the weakest line segment in

the 3-phase feeder structure was established and presented in Figure 4.

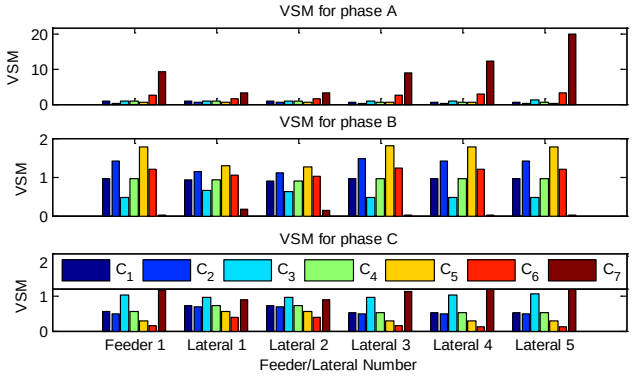

Figure 3. VSM for IEEE 13 Test Feeder for V2G Interconnection at Phase A

The rise in VSI and VSM values on phases B and C relative to Phase A (for Figure 2 and Figure 3) is because of the impact of coupling effect on 3-phase lines, for highly unbalanced systems. This is true for all lightly loaded phases with respect to other phases.

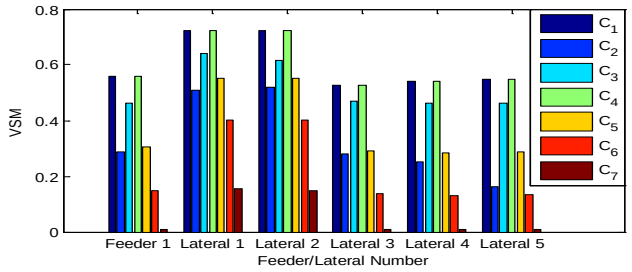

Figure 4. System VSM for V2G Interconnection at Phase A of IEEE 13 System

The respective loading (or power injection) of a phase with respect to other phases are the basis of the differences between phase A, B, C that will result in different VSM outputs.

For all the cases, it is seen that Lateral 2 and Lateral 3 are the 'healthiest' laterals in terms of VSM because the two laterals run lateral from a node nearer to the main source node 650 than the other laterals. Although the main feeder is rooted at the source node, its VSM is expected to be lower because of the nature of loadings on the primary and secondary laterals (Lateral 2, Lateral 3, Lateral 4, Lateral 5 and Lateral 6). It can also be seen that the best VSMs are in Case 1, Case 3 and Case 4, while for any lateral, the lowest VSM is in Case 7. It can be concluded from the results that injecting kW (Case 3) may result in a better VSM than V2G consuming the same amount of kW (Case 2). Lateral 6 (node where the V2G is installed) has the lowest VSM in Case 2, suggesting that increased loading may significantly reduce the VSM at the lateral where the V2G interconnection is installed.

4.1.3. System Voltage Stability Margin

Results presented in Figure 5 show the VSM_{sys} (VSM of the lateral with the lowest value). For all the cases, it is seen that Case 2, Case 6 and Case 7 have the least VSM_{sys}, while Case 1, Case 3, Case 4 and Case 5 have higher VSM_{sys} values.

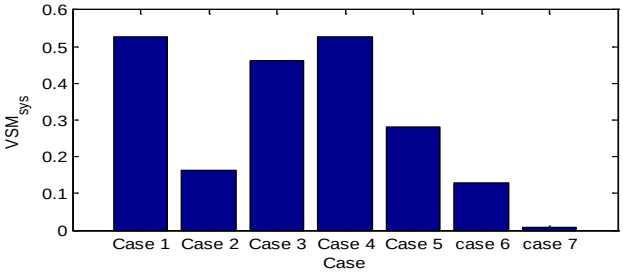

Figure 5. VSM_{sys} for V2G Interconnection at Phase A of IEEE 13 Test Feeder

4.2. Category A: Scenario-2

A 1-phase V2G parking lots unit is interconnected at node N_645 (a Phase B node) to study the effect of V2G on the entire system with respect to VSI and VSM. The results are presented, thus:

4.2.1. Voltage Stability Index

The VSI results for V2G interconnection at Phase B are presented in Figure 6. These results show that significant changes in VSI for the seven different cases took place only at node 632 and node 645. This is because V2G is installed in node 645, which is on a lateral fed by main feeder at node 632. Case 6 significantly increased the VSI of node 632, Phase B.

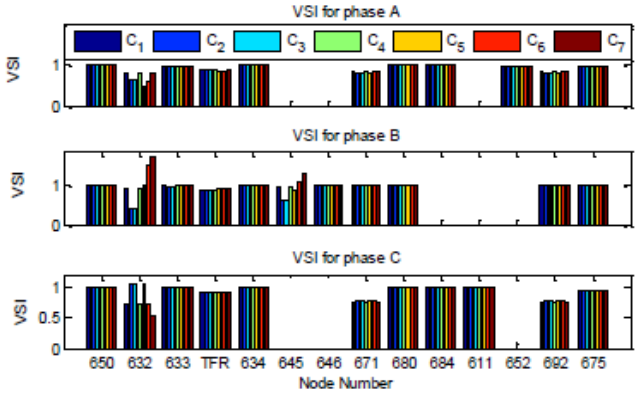

Figure 6. VSI for IEEE 13 Node Test Feeder for V2G Interconnection at Phase B

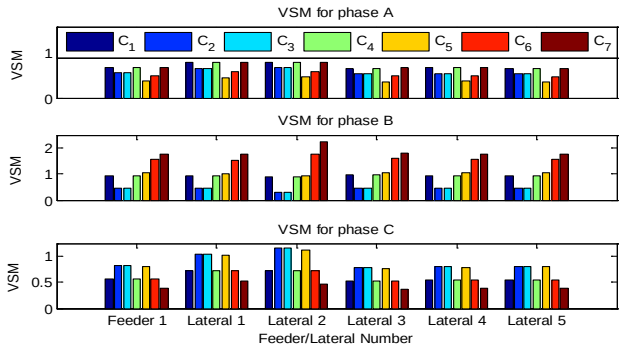

Figure 7. VSM for IEEE 13 Test Feeder for V2G Interconnection at Phase B

4.2.2. Voltage stability margin

The results for the lateral VSM per phase and lateral VSM are presented, respectively, in Figure 7 and Figure 8. From Figure 7, (for all the six laterals), the highest impact

on VSM is made in Case 7 at Phase B. More so, Figure 8 shows that for any lateral or feeder, the maximum VSM in a set of the least VSM (of any number of phases, i.e., computation of (4)) occurred at case 4 and case 6 of lateral 1 and lateral 2. Hence, as in Scenario 1, Lateral 1 and Lateral 2 are the '*strongest*' laterals in terms of VSM, when operated at case 4 and case 6.

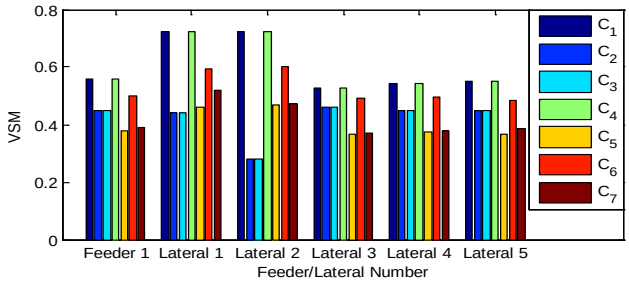

Figure 8. System VSM for V2G Interconnection at Phase B of IEEE 13 System

It may be observed that the '*strongest*' lateral VSM occurred in Case 1, Case 4 and Case 6, while the weakest laterals resulted due to Case 2, Case 3 and Case 5. It can be seen in this case that Case 3 resulted in no better VSM than Case 2 (this is because the level of loading on phase B with respect to other phases). Lateral 3 (lateral where the V2G was installed) has the lowest VSM in Case 2, suggesting that VSM for Case 2 operation is lowest at the node where the V2G interconnection is made.

4.2.3. System Voltage Stability Margin

The results presented in Figure 9 show that the system VSM (VSM of the lateral with the lowest VSM_{sys}) are quite high in Case 4 and Case 6.

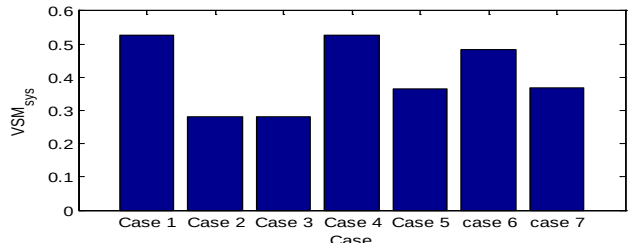

Figure 9. VSM_{sys} for V2G Interconnection at Phase B of IEEE 13 Test Feeder

4.3. Category A: Scenario-3

The V2G facility was installed at node 611 of the IEEE 13 Node Test Feeder system with the aim to investigate how V2G interconnection at Phase C may affect the entire distribution system with respect to voltage profile, VSI, and VSM. (node 611 is a Phase C bus). The simulation results are presented in Figure 10 through Figure 13.

4.3.1. Voltage Stability Index

The VSI results for V2G interconnection at Phase C are presented in Figure 10. As seen, significant changes in VSI took place only at node 632, node 671, node 684 and node 611. This is expected as the V2G is installed at node 611, which is on a lateral fed by lateral 671-684-611. The most significant impact of Case 7 is seen in Phase C.

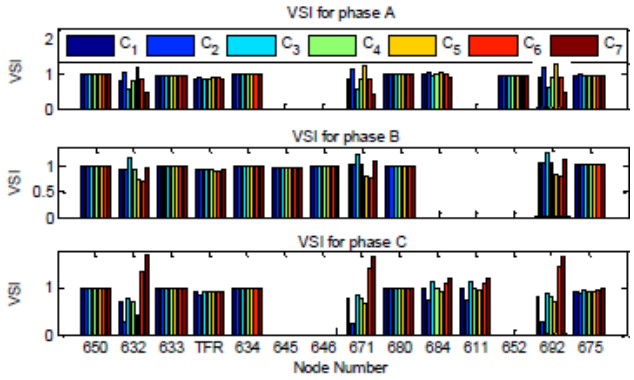

Figure 10. VSI for V2G Interconnection at Phase C of IEEE 13 Test Feeder.

4.3.2. Voltage Stability Margin

The results for the lateral VSM per phase and the lateral VSM are presented, respectively, in Figure 11 and Figure 12. As seen from Figure 11, the highest impact on VSM is made in Case 7 at Phase C. As in Scenario 1 and Scenario 2, Lateral 2 and Lateral 3 have the highest VSM. For any lateral, the best VSM are in Case 1, Case 4 and Case 6. As observed in Scenario 1 and Scenario 2, Case 3 resulted in better lateral VSM than Case 2, while Lateral 5 (node where the V2G installed) has the lowest VSM in Case 2.

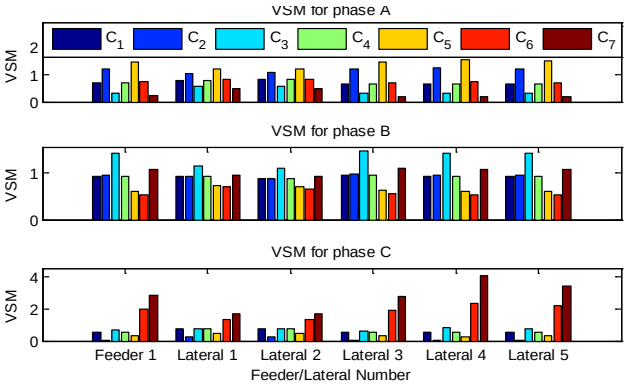

Figure 11. 3-phase VSM for V2G Interconnection at Phase C of IEEE 13 Feeder

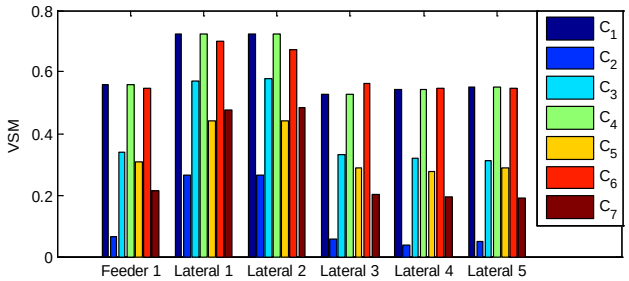

Figure 12. Feeder VSM for V2G Interconnection at Phase C of IEEE 13 Feeder

4.3.3. System Voltage Stability Margin

The results presented in Figure 13 show the system VSM. The results indicate that Case 2 operation would result in a system more prone to system failure than the rest. However, Case 1, Case 4 and Case 6 have high VSM_{sys}.

It was seen that V2G integrations at Phase A and Phase C resulted in better VSM when injecting kW than V2G

consuming kW. This was not the case in Phase B because of its relative loading.

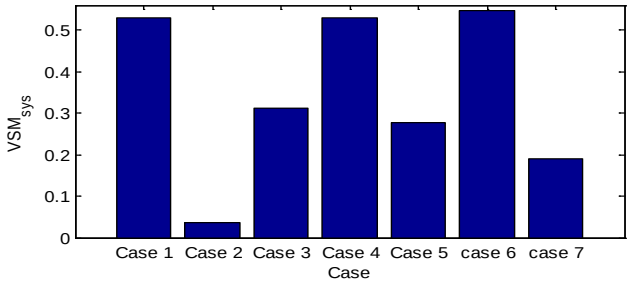

Figure 13. VSM_{sys} for V2G Interconnection at Phase C of IEEE 13 Test Feeder

4.4. Category A: Scenario-4

A 3-phase V2G interconnection was made at node 675 of the IEEE 13 Node Test Feeder system so as to investigate how such a 3-phase facility will affect the entire distribution system with respect to voltage profile, VSI, and VSM. The simulation results are presented from Figure 14 to Figure 17.

4.4.1. Voltage Stability Index

The VSI results for 3-phase V2G interconnection is presented in Figure 14. As seen, the 3-phase interconnection actively affected VS1 at nodes that trace power flow from substation to the node where the V2G is installed (in this case, node 675). This is expected since the V2G is installed at node 675 on Lateral 4, fed by the main feeder.

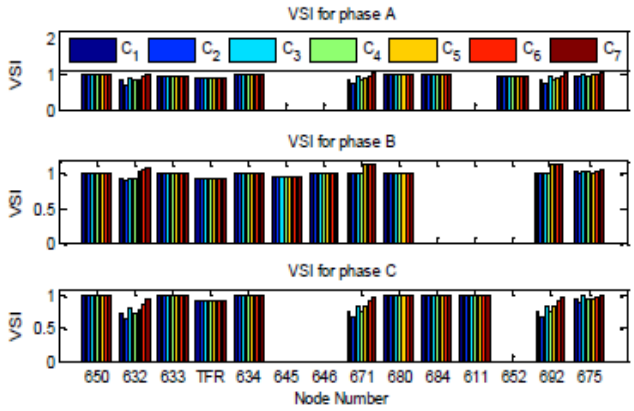

Figure 14. VSI for 3-phase V2G Interconnection of IEEE 13 Test Feeder

4.4.2. Voltage Stability Margin

Results for the 3-phase lateral VSM and the lateral VSM are presented, respectively, in Figure 15 and Figure 16. Again, the results in Figure 15 indicate a more balanced system than the scenarios presented earlier. It may be concluded from Figure 16 and Figure 17 that the '*healthiest*' lateral VSM and '*healthiest*' system VSM are in Case 3, Case 5, Case 6 and Case 7. It can also be observed from Figure 17 that 3-phase V2G integration gave VSM greater than the VSM of the original system (Case 1), which is an improvement in the system security. It is further observed that the improved system VSM took place at the lateral where power is injected into the distribution system, with the highest impact made in Case 7. The contrast took place in Case 2, where all the V2G in the system are operated in demand mode.

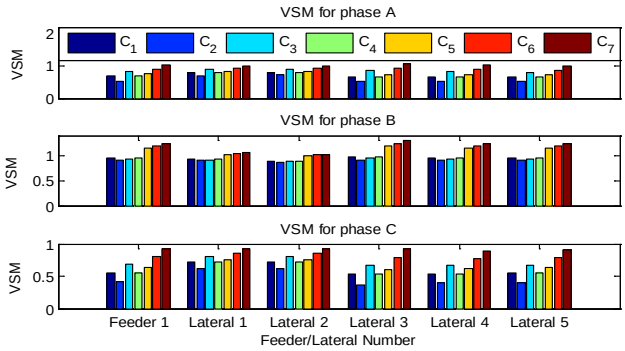

Figure15. VSM of Laterals for 3-phase V2G Interconnection of IEEE 13 Feeder

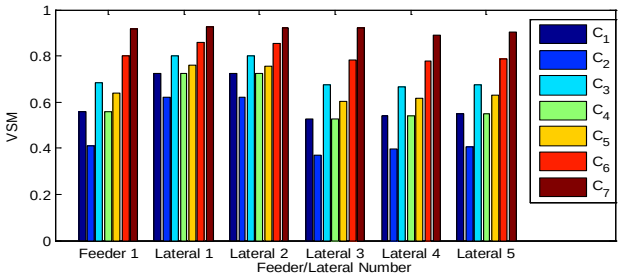

Figure 16. Lateral VSM for 3-phase V2G Interconnection of IEEE 13 Feeder

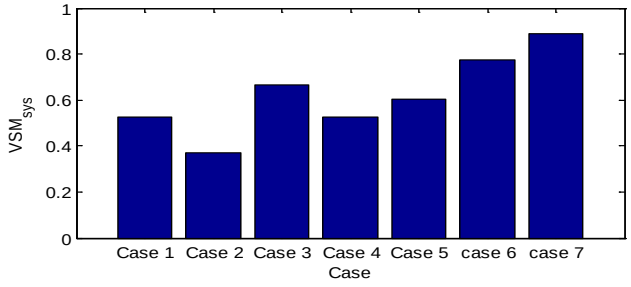

Figure 17. VSM_{sys} for 3-phase V2G Interconnection of IEEE 13 Test Feeder

4.5. Category B: Scenarios 5, 6, 7, 8, and 9

So far, in Category A, study of V2G penetration in the IEEE test system was to investigate how the V2G interconnection at a single node affects the entire system by injecting or consuming power. It is expedient, however, to investigate how a wide spread use of the V2G facilities in the entire system affects the distribution system performance. This consideration will mimic the real life situation where a mix of both 3-phase, 2-phase and single-phase V2G facilities may be installed at many parts of the distribution system. To implement this, a percentage of the total system load was injected or demanded at each of the *9* load bus nodes for the IEEE 13 test system (namely, 634, 645, 646, 652, 671, 675, 692, 611 and 632), such that the total power injected was either 2500 kW or 2500 kvar, or such that the total power consumed was 2500 kW. The load busses are made up of 8 spot load and a distributed load [13]. The total system kW load in the IEEE 13 Node Test is 3466 kW, while the total system kvar is 2102 kvar. Hence, installing V2G capacity of 2500 kW would imply

about 72% additional kW load or injection, while 2500 kvar V2G capacity corresponds to 119% of total system kvar load. The justification for this analysis is to make credible comparison and conclusions between the impact of *single-node* V2G interconnection and *multi-node* interconnection on the system. In Scenario 5, 2500 kW V2G-load was added to the entire distribution system at all load buses (1-phase and 3-phase spot load buses alike) to investigate the effect of such V2G loading on the entire system. In Scenario 6, 2500kW of V2G power was injected to the entire system at the load buses, while in Scenario 7, V2G consuming 2500 kW power and injecting 2500 kvar of reactive power is investigated. Scenario 8 presents the situation whereby only 2500 kvar of V2G reactive power was injected to the entire system at load buses. Finally, V2G simultaneously injecting 2500 kW and 2500 kvar power was considered in Scenario 9. It was assumed that all the spot load buses have a V2G facility. Voltage stability is discussed next.

4.5.1. Voltage Stability Index

The VSI results for Category B V2G interconnection are presented in Figure 18. The results indicate that Category B interconnection significantly affected VS1 at node 632 and 671 (nodes on the main feeder feeding the laterals).

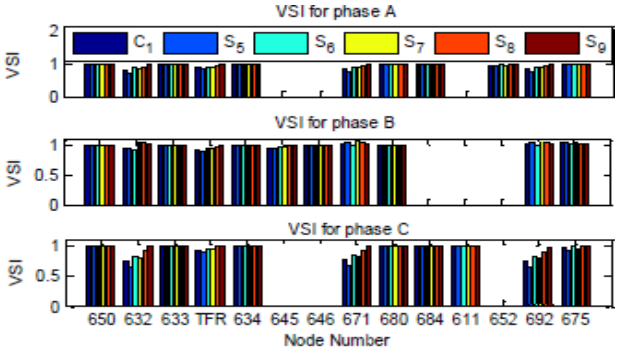

Figure 18. VSI for Category B V2G Interconnection of IEEE 13 Test Feeder

4.5.2. Voltage Stability Margin

The results for the 3-phase lateral VSM, the lateral VSM and system VSM are presented in Figure 19 through Figure 21, respectively. Results in Figure 19 indicate a near-balanced system loading, similar to the Scenario 4 results. From Figure 20 and Figure 21, it is discovered that the highest VSM magnitude occurred at Scenario 9. A comparison of VSM between different cases and scenarios is presented in Table 3. From Table 3, it is seen that VSM for Scenario 9 of Category B is 0.9803, thereby resulting in about 10% increase in VSM when compared with the VSM of 3-phase integration at Case 7 (Case 7 in Category A is operationally equivalent to Scenario 9 in Category B). For the sake of clarity, if VSM_B/VSM_A denotes VSM of Category B entries with respect to the corresponding VSM in Scenario 4 entries of Category A, then it implies from Table 3 that the set of VSM_B/VSM_A may be defined as

$$\frac{VSM_B}{VSM_A} = \left[\underset{\substack{\uparrow \\ \frac{C_2}{Scenario5}}}{\frac{0.3734}{0.3701}} \quad \underset{\substack{\uparrow \\ \frac{C_3}{Scenario6}}}{\frac{0.6816}{0.6646}} \quad \underset{\substack{\uparrow \\ \frac{C_5}{Scenario7}}}{\frac{0.6017}{0.6045}} \quad \underset{\substack{\uparrow \\ \frac{C_6}{Scenario8}}}{\frac{0.7928}{0.7765}} \quad \underset{\substack{\uparrow \\ \frac{C_7}{Scenario9}}}{\frac{0.9803}{0.8911}}\right] \quad (5)$$

The above equation simply implies that Category B offers more improvement in the system security than Scenario 4 of Category A (except in the third entry where very close magnitudes exist for both categories). A closer look at Table 3 indicates that Scenario 4 has the best VSM in Category A; hence, Category B has the global best system VSM. This finding is important since system security has become a topical issue in power system operation.

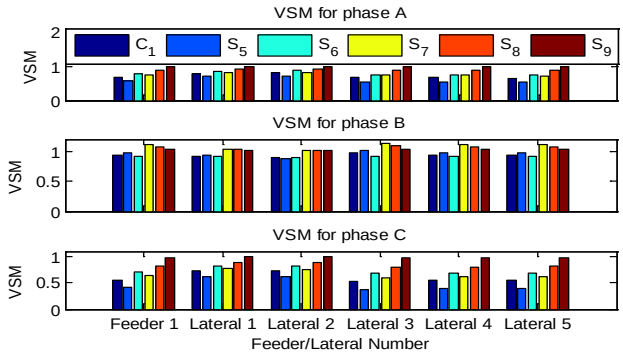

Figure 19. 3-Phase VSM for Category B V2G Interconnection of IEEE 13 Feeder

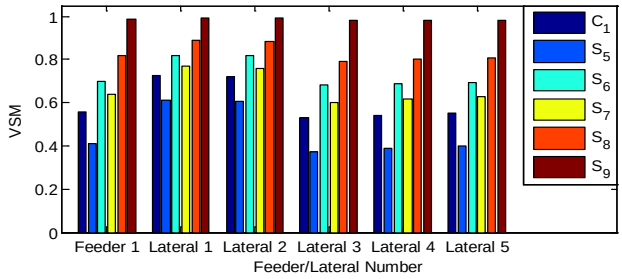

Figure 20. System VSM for Category B V2G Interconnection of IEEE 13 Feeder

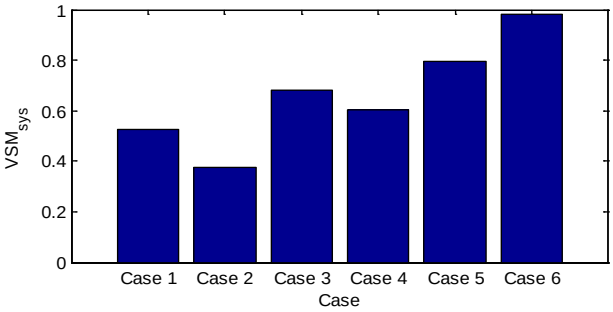

Figure 21. System VSM for Category B V2G Interconnection of IEEE 13 Feeder

Table 3. Summary of IEEE 13 Test Node system VSM

Scenario	Case						
	Case 1	Case 2	Case 3	Case 4	Case 5	Case 6	Case 7
1	0.5282 *(4)	0.1620 (6)	0.4615 (1,5,6)	0.5285 (4)	0.2824 (6)	0.1297 (5)	0.0093 (1,5,6)
2	0.5285 (4)	0.2816 (3)	0.2816 (3)	0.5285 (4)	0.3657 (6)	0.4838 (6)	0.3695 (4)
3	0.5285 (4)	0.0358 (5)	0.3124 (6)	0.5285 (4)	0.27690 (5)	0.5469 (6)	0.1888 (6)
4	0.5285 (4)	0.3701 (4)	0.6646 (5)	0.5285 (4)	0.6045 (4)	0.7765 (5)	0.8911 (5)
5	0.3734 (4)						
6	0.6816 (4)						
7	0.6017 (4)						
8	0.7928 (4)						
9	0.9803 (4)						

*Bracketed entries are the pivotal feeders where the system VSM occurred.

4.6. Category C: Scenario 10

V2G power multiplier factor was introduced in Category C study with the aim to establish a relationship between VSM and V2G power multiplier factor. The V2G power multiplier factor is a quantification of V2G power in terms of how many times the system loading is the V2G injecting or consuming in the entire network. The three investigations made here are: V2G demanding kW in multiples of system kW load, V2G injecting kW in multiples of system kW load and V2G injecting kvar in multiples of system kvar load. The designation V2G-kW$_{_DMF}$ represents V2G kW load demand multiplier factor, while V2G-kW$_{_IMF}$ and V2G-kvar$_{_IMF}$ represent V2G kW power injection multiplier factor and V2G kvar power injection multiplier factor, respectively. For instance, kW-$_{DMF}$ of 1.5 would mean that V2G is consuming 1.5 times the total system kW load (total system kW load for IEEE 13 test feeder system is 3466 kW), while kvar$_{_IMF}$ of 2.5 means that 2.5 times the total system kvar load is injected into the entire system(total system kvar load being 2102 kvar). The manner in which VSM is impacted by the V2G-kW$_{_DMF}$, V2G-kW$_{_IMF}$ and V2G-kvar$_{_IMF}$ are summarized in Figure 22 through Figure 25. Figure 22 indicates that the VSM versus V2G-kW$_{DMF}$ is a linear relationship with negative gradient. Hence, increasing the load multiplying factor will lead to decreasing VSM. This explains why VSM in all the scenarios decreased with 2500 kW loading. Lateral 4 has the lowest VSM for all the load levels, and is therefore considered the weakest lateral in the system (the VSM of Lateral 4 is 0.5285). Table 3 also indicates that in all Scenarios (1 through 9), the dominant lateral with the lowest VSM is Lateral 4. This result agrees with the result of a similar independent study in which balanced system was assumed for the distribution system [12]. Using linear extrapolation, the VSM corresponding to any V2G-kW$_{_DMF}$ can be calculated and is presented in Figure 22.

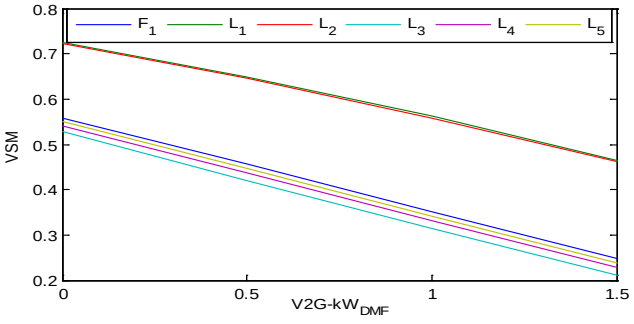

Figure 22. Variation of VSM of all laterals of 13-Node system with kW$_{_DMF}$

Since voltage collapse point for each lateral is defined as the operating point where $VSM(x) = 0$, it is possible to calculate the critical value V2G-kW$_{_DMF}$ (i.e.,x) corresponding to the voltage collapse point as

$$x = x_a - \frac{VSM_a\left(x_b - x_a\right)}{VSM_b - VSM_a} \quad (6)$$

The result of computing *critical V2G-kW$_{DMF}$* for different laterals of the IEEE 13 system is presented in Figure 23. The lateral corresponding to the least value of *critical V2G-kW$_{_DMF}$* is actually the weakest lateral, and its *critical V2G-kW$_{_DMF}$* is the system *critical V2G-kW$_{_DMF}$*.

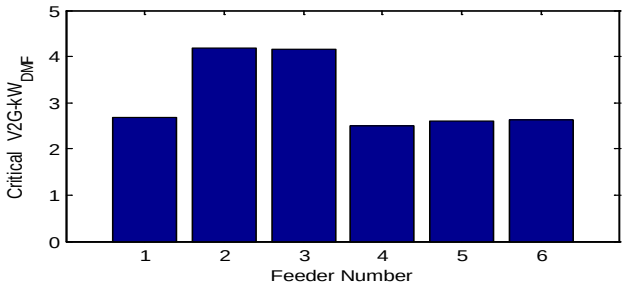

Figure 23. *V2G-kW$_{DMF}$* required to initiate voltage collapse for IEEE 13 Feeder.

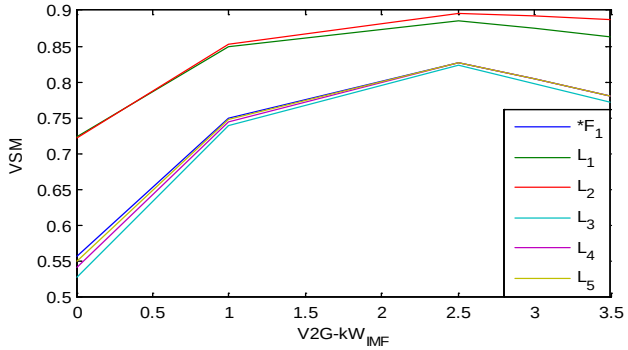

Figure 24. Variation of VSM of all laterals of 13-Node system with kW$_{_IMF}$

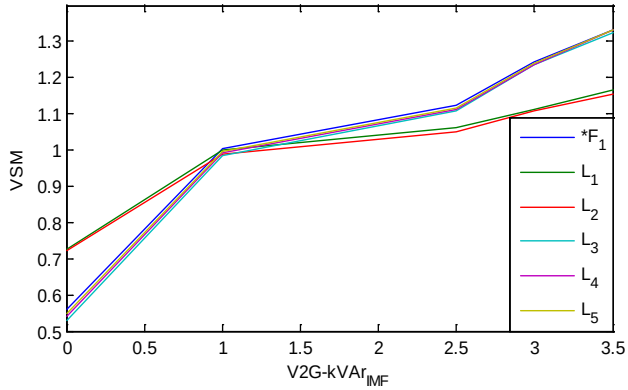

Figure 25. Variation of VSM of all laterals of 13-Node system with kvar$_{_IMF}$

Hence, the system *critical V2G-kW$_{DMF}$* is 2.4962. In this study, the *V2G-kW$_{_DMF}$* was successively increased at a uniform rate and solving the power flow problems using RDAP until convergence failed. It was observed that at any value beyond *V2G-kW$_{_DMF}$* =2.5, the RDAP failed to converge the power flow iteration (notice that the *critical system V2G-kW$_{DMF}$* is 2.4962, which is approximately 2.5). This shows that the estimated *critical V2G-kW$_{_DMF}$* for the system is actually the least of the estimated *critical V2G-kW$_{_DMF}$* for all the laterals. On the other hand, it can be seen in Figure 24 and Figure 25 that successively injecting kW (V2G-kW$_{IMF}$) or injecting kvar (V2G-kvar$_{IMF}$) resulted in a different characteristic. Figure 24 shows that injecting kW increased the VSM of all the laterals to a limit, beyond which their VSM starts to decrease. Figure 25 indicates that successively injecting same amount of kvar results in increasing VSM of all the laterals. It is may also be observed in Figure 25 that injecting equal amount of kvar into the system resulted in higher magnitudes of VSM. This characteristic implies that injecting kvar has more impact on VSM than injecting equal amount of kW power. This further explains why significant improvements

in VSI took place in Scenario 4 (Cases 3, 6, 7) and Scenarios 6, 8, 9. In these cases and scenarios, kvar was injected.

From the investigations made in this study, it is evident that case studies dealing with the charging of V2G reveal reduced voltage stability, while cases for power injection do the contrary. However, kvar power injection improves the system stability more than kW injection.

5. Conclusions

The impact of V2G on voltage stability of IEEE 13 test node feeder system was studied. The simulation results show that 3-phase spot integration and system-wide (i.e., Category B) V2G integration will result in an improved voltage stability performance than the 1-phase integration. The operational relationship between VSM and V2G capacity was investigated, and results show that V2G parking lots injecting reactive power will have more impact on the voltage stability of the system than injecting a real power into the system. Hence, operating the distribution system in 3-phase modes and/or balanced system wide operation, while taking additional advantage of kW or kvar power injections is highly recommended. The study may offer useful tool for real-time applications as the smart grid initiative takes prominence.

References

[1] Saber, A.Y., Venayagamoorthy, G.K., "Optimization of vehicle-to-grid scheduling in Constrained parking lots." *PES GM*, pp.1-8. 2009.

[2] M. Duvall. "Comparing the Benefits and Impacts of Hybrid Electric Vehicle Options for Compact Sedan and Sport Utility Vehicles, *EPRI*, Palo Alto, CA, Final Report 1006892. 2002.

[3] V. Ajjarapu and B. Lee. "Bibliography on voltage stability, *IEEE Trans. on power systems," Vol. 13*, pp. 115-125, 1998.

[4] T. Gonen, "Electric Power Distributed System Engineering," 2nd Ed. New York: McGraw-Hill, pp. 414-435, 1987.

[5] P. Nagendra, T. Datta, S. Halder and S. Paul. "Power system stability assessment using Network Equivalents- A Review," *Journal of applied sciences*, Vol. 10, Iss 18, pp. 2147-2153, 2010.

[6] P. Kundur. *Power system stability and control*, McGraw-Hill, 1st Ed.

[7] B. Gao, G. K. Morison, and P. Kundur. "Voltage stability evaluation using Modal analysis," *IEEE trans. on power systems, Vol. 7, Iss* 4, pp. 1529-1542, 1992.

[8] V. Ajjarapu and C. Christy, "The continuation power flow: A tool for steady State voltage stability analysis," *IEEE Trans on power systems, 7*(1), pp. 416-423, 1992.

[9] C. A. Canizares. Voltage stability assessment: concepts, practices & tools. *IEEE-PES Power systems stability subcommittee publication*.

[10] D.O. Dike, S.M. Mahajan, "Utilization of L-index in microgrid interconnected power system network, *proceedings of the IEEE PES GM*, 1-6, 2008.

[11] P. Aravindhababu and G. Mohan "Optimal Capacitor Placement for Voltage Stability Enhancement in Distribution Systems," *ARPN Journal of Engineering and Applied Sciences* Vol. 4, No. 2, 88-92, 2009.

[12] M. H. Haque, "A linear static voltage stability margin for radial distribution systems," *in Proc. IEEE PES GM, Quebec* pp. 1-6, 2006.

[13] [Online]http://www.ewh.ieee.org/soc/pes/dsacom/testfeeders.html.

[14] G. Mohan and P. Aravindhababu. Load shedding Algorithm for avoiding Voltage instability in distribution systems, *Int. J. of Power Engineering and Green Technology (IJPEGT)*, Vol. 1. Iss. 1, pp. 39-45. 2010.